The Journal of Immunology

Inhibition of PI3Kδ Reduces Kidney Infiltration by Macrophages and Ameliorates Systemic Lupus in the Mouse

Abel Suárez-Fueyo, José M. Rojas, Ariel E. Cariaga, Esther García, Bart H. Steiner, Domingo F. Barber, Kamal D. Puri and Ana C. Carrera

J Immunol 2014; 193:544-554; Prepublished online 16 June 2014;
doi: 10.4049/jimmunol.1400350
http://www.jimmunol.org/content/193/2/544

The Journal of Immunology is published twice each month by
The American Association of Immunologists, Inc.,
1451 Rockville Pike, Suite 650, Rockville, MD 20852

Print ISSN: 0022-1767 Online ISSN: 1550-6606.

Inhibition of PI3Kδ Reduces Kidney Infiltration by Macrophages and Ameliorates Systemic Lupus in the Mouse

Abel Suárez-Fueyo,* José M. Rojas,* Ariel E. Cariaga,* Esther García,† Bart H. Steiner,‡ Domingo F. Barber,* Kamal D. Puri,‡ and Ana C. Carrera*

Systemic lupus erythematosus (SLE) is a human chronic inflammatory disease generated and maintained throughout life by autoreactive T and B cells. Class I phosphoinositide 3-kinases (PI3K) are heterodimers composed of a regulatory and a catalytic subunit that catalyze phosphoinositide-3,4,5-P_3 formation and regulate cell survival, migration, and division. Activity of the PI3Kδ isoform is enhanced in human SLE patient PBLs. In this study, we analyzed the effect of inhibiting PI3Kδ in MRL/*lpr* mice, a model of human SLE. We found that PI3Kδ inhibition ameliorated lupus progression. Treatment of these mice with a PI3Kδ inhibitor reduced the excessive numbers of $CD4^+$ effector/memory cells and B cells. In addition, this treatment reduced serum TNF-α levels and the number of macrophages infiltrating the kidney. Expression of inactive PI3Kδ, but not deletion of the other hematopoietic isoform PI3Kγ, reduced the ability of macrophages to cross the basement membrane, a process required to infiltrate the kidney, explaining MRL/*lpr* mice improvement by pharmacologic inhibition of PI3Kδ. The observations that p110δ inhibitor prolonged mouse life span, reduced disease symptoms, and showed no obvious secondary effects indicates that PI3Kδ is a promising target for SLE. ***The Journal of Immunology*****, 2014, 193: 544–554.**

Systemic lupus erythematosus (SLE) is a complex multigenic disease caused by autoreactive T and B cells (1). This chronic inflammatory process affects ∼1 in 1000 whites, with even higher frequencies in blacks, Native Americans, and Asians (90% of patients are females) (1–3). Current immunosuppressive therapy based on long-term corticosteroid treatment presents side effects (4, 5); it is thus important to develop therapeutic approaches that are more specific. In both human and murine lupus, autoreactive B and T cell numbers are increased, and there is accumulation of long-lasting $CD4^+$ memory cells, which include the autoreactive T cells responsible for disease maintenance throughout life (6–8).

Patients with SLE have large amounts of serum autoantibody produced by activated autoreactive B cells (9, 10). SLE affects various organs, including the kidney (in 60% of cases), which is also the most affected organ in the mouse model (11–13). Kidney dysfunction, the primary cause of fatal lupus, is provoked by the deposition of circulating autoantibodies that activate the complement cascade (12). T cells and macrophages also infiltrate the kidney and support local inflammation, producing renal failure at advanced stages (12–15). The correlation of macrophage infiltration and kidney dysfunction in humans supports the contribution of macrophages in lupus (12, 14). Macrophages also invade the mouse kidney; CSF-1– or MCP-1–deficient mice that lack kidney macrophage infiltrates present less severe disease (12, 14, 16–18). Various B and T cell defects are reported in SLE, including altered BCR and TCR signaling, reduced IL-2 production by T cells, COX-2 upregulation, and increased PI3K activation (19–24). Deregulation of T and B cells and kidney infiltration by macrophages are thus thought to be critical events in SLE progression.

Class I PI3K are heterodimers composed of a p110 catalytic (p110α, p110β, p110δ, or p110γ) and a regulatory subunit. p85 regulatory subunits associate with p110α, β, and δ, whereas p87 and p101 regulatory subunits bind to p110γ. PI3K catalyze the formation of phosphoinositide-3,4,5-P_3 (PIP_3) and, following the action of SHIP 5′ phosphatase, of phosphoinositide 3,4-P_2. These lipids initiate activation of downstream effector molecules such as Akt, which triggers cell survival (25–27). p110α and p110β are ubiquitous, whereas p110δ and p110γ are more abundant in cells of hematopoietic origin. In the mouse, p110α or p110β deficiency is lethal at the embryonic stage, whereas p110δ or p110γ deletion impairs immune responses (25, 28). Indeed, p110δ deletion reduces T cell activation and B cell differentiation as well as the allergic response (29, 30), whereas p110γ deficiency impairs T cell activation as well as macrophage and neutrophil migration (31, 32).

Expression in T cells of a p85 mutant ($p65^{PI3K}$) that mediates enhanced PI3K activation is sufficient to trigger systemic lupus-like disease in the mouse (24). The phenotype is similar to the deletion of the negative regulator of the PI3K pathway, the phosphatase PTEN (33). Inhibition or deletion of p110γ in lupus-prone mice alleviates disease symptoms (34, 35), suggesting that this isoform might be useful for SLE treatment. Study of the PI3K

*Departamento de Inmunología y Oncología, Centro Nacional de Biotecnología/Consejo Superior de Investigaciones Científicas, Cantoblanco, Madrid 28049, Spain; †Departamento de Biologia Molecular e Celular, Centro Nacional de Biotecnología/Consejo Superior de Investigaciones Científicas, Cantoblanco, Madrid 28049, Spain; and ‡Department of Biology, Gilead Sciences, Seattle, WA 98102

Received for publication February 5, 2014. Accepted for publication May 12, 2014.

This work was supported by a predoctoral fellowship from the Carlos III Institute of the Spanish Ministry of Health (A.S.F), a Junta de Ampliación de Estudios Doctoral program contract from the Spanish Ministry of Economy and Competitiveness cofinanced by the European Social Fund (J.M.R.), and grants from the Spanish Ministry of Science and Innovation (SAF 2007-63624, SAF2010-21019, SAF2011-23639), the Network of Cooperative Research from the Carlos III Institute of Health (RD07/0020/2020, RD08/0075/2015, and RD12/0036/0059), and the Madrid Regional Government.

Address correspondence and reprint requests to Prof. Ana Clara Carrera, Departamento de Inmunología y Oncología, Centro Nacional de Biotecnología/Consejo Superior de Investigaciones Científicas, Darwin 3, Campus de Cantoblanco, Madrid 28049, Spain. E-mail address: acarrera@cnb.csic.es

The online version of this article contains supplemental material.

Abbreviations used in this article: AICD, activation-induced cell death; BMDM, bone marrow–derived macrophage; PIP_3, phosphoinositide-3,4,5-triphosphate; SLE, systemic lupus erythematosus; Treg, regulatory T cell; TR-FRET, time-resolved fluorescence resonance energy transfer.

pathway in SLE patient peripheral blood cells nonetheless showed that p110δ is the isoform most frequently activated in human patients (36). The consequences of p110δ inhibition for lupus development in vivo are incompletely understood. The lupus disease in MRL/*lpr* mice resembles human SLE in that it is caused by the combined action of several susceptibility alleles (37). In this study, we tested the effect of p110δ inhibition in MRL/*lpr* lupus-prone mice.

Materials and Methods

GS-9829 structure, in vitro PI3K activity assays, and GS-9829 selectivity assays

GS-9829 (formerly CAL-129) was provided by Calistoga Pharmaceuticals (a wholly owned subsidiary of Gilead Sciences, Foster City, CA); for the chemical structure, see Fig. 1A. We tested GS-9829 inhibitory potency (IC50) on class I PI3K isoforms using a time-resolved fluorescence resonance energy transfer (TR-FRET) assay (38) that monitors PIP_3 formation; PIP_3 in each sample competes with fluorescently labeled PIP_3 for binding to the GRP-1 pleckstrin homology domain. Class I PI3K isoforms were expressed and purified as heterodimeric recombinant proteins. All assay reagents were purchased from Millipore. Purified p110α, p110β, and p110δ (25–50 pM) as well as p110γ (2 nM) were assayed in initial rate conditions in kinase buffer (25 mM HEPES pH 7.4, 2 μM PIP_2, 5% glycerol, 5 mM $MgCl_2$, 50 mM NaCl, 0.05% (v/v) CHAPS, 1 mM DTT, and 1% [v/v] DMSO), at an ATP concentration of twice the K_m for ATP of each enzyme. Reactions proceeded for 30 min at 25˚C and were terminated by adding 10 mM EDTA, 10 nM PIP_3, and 35 nM europium-labeled GRP-1 detector protein. TR-FRET was estimated on an Envision plate reader (Ex: 340 nm; Em: 615/665 nm; 100 μs delay and 500 μs read window). IC_{50} values were calculated as dose-response curves. All IC_{50} values are the geometric mean of at least four assays (Fig. 1A, Table I). GS-9829 (10 μM) selectivity was tested in an ATP-binding competition assay using a panel of 442 kinases (KinomeScan; Ambit Biosciences) (39) (Supplemental Fig. 1). GS-9829 was considered active for a kinase when the kinase fraction that remained bound to ATP was <30%.

Cell-based GS-9829 inhibitory assays and analysis of serum GS-9829 levels

To study GS-9829 selectivity on class I PI3K isoforms in cell-based assays, we measured Akt phosphorylation (Ser473) in murine embryonic fibroblasts incubated in serum-free medium (2 h), followed by stimulation with platelet-derived growth factor (10 ng/ml PDGF [Cell Signaling], 10 min, 37˚C) for p110α or with LPS (10 μM LPA [Echelon], 10 min, 37˚C) for p110β (40). p-Akt and Akt levels in cell extracts were analyzed by Western blot. To analyze inhibition by GS-9829 of p110δ and p110γ, we measured basophil activation in isolated PBMCs using the Flow2-CAST kit (Bühlmann Laboratories; human p110δ and p110γ proteins were 95% and 94% identical, respectively, to mouse isoforms and >95% conserved). Blood samples were obtained with informed consent according to the Helsinki declaration, and PBMCs were isolated by filtration-capture (WBF-2 filter; Pall Biomedical). For p110δ activation, cells were treated with anti-FcεRI Ab (Millipore). *N*-formyl-L-methionyl-L-leucyl-L-phenylalanine for p110γ were used. To monitor basophil activation alone or after incubation with GS-9829, we analyzed CD63-FITC and CCR3-PE (BD Biosciences) staining on an FC500MPL flow cytometer. Dose-response curves to estimate the GS-9829 IC50 for each isoform (Fig. 1A, Table II) were used.

GS-9829 concentration in serum was determined after liquid-liquid extraction by liquid chromatography–mass spectroscopy (Fig. 1B). The lower quantification limit was 1 ng/ml.

Abs and reagents

We used rabbit polyclonal anti–phospho-Thr308-Akt, phospho-Ser473, -Akt, -p110β -p110α (Cell Signaling), and anti–β-actin (Sigma-Aldrich) for Western blot. Rabbit anti-p110γ was obtained from Santa Cruz Biotechnology, and rabbit anti-p110δ was obtained from Abcam. For flow cytometry, Abs conjugated to appropriate fluorochromes for CD3 (145-2C11), CD4 (L3T4, H129.19), CD8 (Ly-2, 53-6), CD44 (pgp1, IM7), CD11b, B220 (Becton Dickinson), F4/80 (Serotec), and CD62L (Pharmingen) were used. Peanut oil was obtained from Sigma-Aldrich.

Mouse treatment

MRL/*lpr* mice were maintained in the Centro Nacional de Biotecnología animal facility. The CNB Ethics Committee approved all studies in accordance with European Union legislation (Directive 2010/63/EU).We inhibited p110δ with GS-9829 (30 mg/kg) dissolved in peanut oil (stock at 7.5 mg/ml); controls were treated with vehicle (peanut oil). Vehicle and GS-9829 were administered orally every 12 h. In experiment 1, mice were treated from month 3 to month 5.5. We included two groups in experiments 2 and 3, with treatment starting at month 3 or 3.5 and finishing at month 5.5, at which time some untreated mice showed renal failure. For bone marrow–derived macrophages (BMDMs), $p110\gamma^{-/-}$ and $p110\gamma^{+/-}$ (31) or $p110\delta^{WT/WT}$ and $p110\delta^{D910A/D910A}$ mice (29) were maintained in pathogen-free conditions. BMDMs were obtained from 3–4-mo-old $p110\gamma^{-/-}$ and $p110\gamma^{+/-}$ or $p110\delta^{WT/WT}$ and $p110\delta^{D910A/D910A}$ littermates, using a modification of a previously described method (41). Briefly, bone marrow cells were cultured with 50 ng/ml recombinant mouse M-CSF (Peprotech) in bacterial grade 100-mm plastic plates (4–5 d). Nonadherent cells were then discarded, and adherent cells were cultured with fresh medium containing 50 ng/ml M-CSF until day 7. Purity and expression of macrophage markers was assessed with flow cytometry. M-CSF was removed from the culture on day 7 for 24 h to synchronize the BMDMs, and cells were plated on basement membranes as described below.

Basement membrane assay

Basement membrane from murine peritoneum was isolated as described (42). The membrane was obtained from the mouse peritoneum and transferred to the plastic cup of a Boyden chamber (with the filter removed), and edges were sealed with a 50:50 wax-paraffin mixture. The membrane was treated with 0.2 mM ammonium hydroxide (1 h, room temperature), followed by three washes with ice-cold PBS. The Boyden chamber with the basement membrane was placed in a 24-well plate containing 50 ng/ml M-CSF (Peprotech) and 3×10^5 macrophages seeded onto the membrane (100 μl) and incubated (3 d, 37˚C). Cells were fixed with 4% formaldehyde, permeabilized with 0.05% Triton X-100, and incubated with rabbit anti-collagen IV (1:200, 100 μl; ab19808 Abcam) for 30 min. After washing with PBS, cells were incubated with goat anti-rabbit (1:500; A594), Alexa 488-labeled phalloidin (1:500), and DAPI (1:200; 45 min). Cells were washed three times with PBS and stored at 4˚C. Membrane cultures were performed in duplicate, and three to six random fields were acquired for each culture. For imaging, PBS was removed, Fluoromount-G added (Southern Biotech) and images acquired on a Leica TCS SP5 confocal microscope with a 40×/1.25 NA oil objective and recorded with a three-channel PMT detector. Collagen IV degradation was measured by projection of all z-planes acquired and quantified with ImageJ software. Cell numbers in basement membrane layers were enumerated with ImageJ using the DAPI-captures in z-planes for the bottom, center, or top membrane section (cumulative data, $n = 4$).

We assessed the cytotoxic effects of PI3K inhibitors on BMDMs differentiated from C57BL/6J mice (day 7). BMDMs were cultured with DMSO, GS-9829, or AS-605240 (PI3Kγ-specific inhibitor) (43) at 10, 1, or 0.1 μM for 3 d. Cultures were supplemented with inhibitors every 12 h to mimic in vivo drug delivery. Cells were harvested at 24, 48, and 72 h, and viability was assessed with flow cytometry using annexin-V–FITC (Beckman) and 7-amino-actinomycin D staining. To analyze the effect of isoform-specific PI3K inhibition on BMDM invasion of basement membranes, BMDMs were allowed to invade for 3 d in the presence of 0.2 μM GS-9829, 1 μM AS-605240, or DMSO, renewed every 12 h. After 72 h, cells were fixed with 4% paraformaldehyde in PBS, and collagen IV degradation and BMDM position in the membrane were analyzed as above.

Flow cytometry analysis, cell preparation

Spleen and lymph node cell suspensions were prepared as described previously (34). For cytometry, 10-color immunofluorescence in a Gallios flow cytometer (Beckman Coulter) were used. Regulatory T cells (Tregs) were detected using the Treg Bioscience Kit. Cells for Th17 staining were prestimulated with 50 ng/ml PMA and 1 mg/ml ionomycin (4 h) in the presence of 2 μg/ml brefeldin A, and then fixed and permeabilized using Intraprep (Beckman Coulter).

Biochemical and serological analyses and cytokine production

Cell extracts were prepared in lysis buffer containing 1% Triton-X100 and Western blot was performed as described (36). We evaluated PI3K pathway activation in cell extracts by analyzing phosphorylation of the PI3K effector Akt using an anti–p-Akt Ab (Thr 308; Cell Signaling) (36). p-Akt, Akt, and actin levels were assessed with Western blot. The p-Akt signal was normalized to that of Akt. Serum Ig, isotype-specific anti-dsDNA Ab and urine protein levels were measured as described (24, 34). Mice were examined daily. When severe SLE symptoms appeared, affected mice were sacrificed and organs were collected for histologic analysis, Western blot,

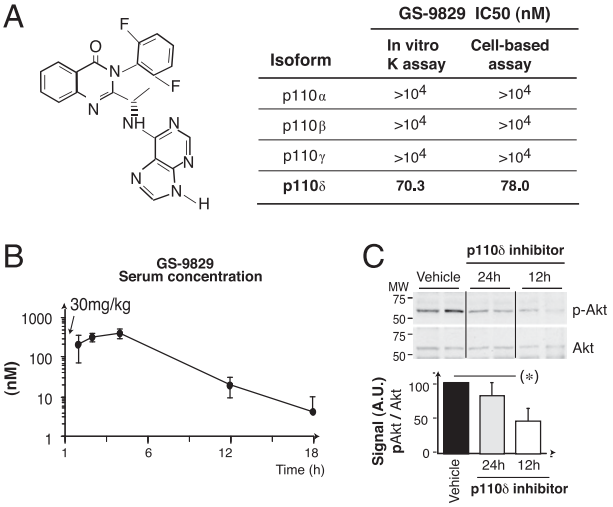

FIGURE 1. GS-9829 selectively blocks p110δ in vivo. (**A**) GS-9829 structure. The table shows IC_{50} values of GS-9829 (nanomolar concentration for 50% inhibition) for the indicated purified p110 isoforms in a FRET-based assay to measure PIP_3 production. GS-9829 selectivity was also tested in cell-based assays (see *Materials and Methods*). GS-9829 IC_{50} was estimated for each isoform using dose-response curves. IC_{50} values shown are the geometric mean of at least three determinations. (**B**) The graph shows the GS-9829 concentration in MRL/*lpr* mouse serum at various times after initial treatment ($t = 0$) with a single dose of GS-9829 (30 mg/kg). (**C**) MRL/*lpr* mice were treated orally every 12 or 24 h with GS-9829 (30 mg/kg) for 3 d, left untreated for 12 or 24 h and then examined. Splenocyte extracts were analyzed in Western blot. The graph shows p-Akt signal normalized to cell Akt levels (mean ± SD; $n = 4$). *$p < 0.05$, Student t test. A.U., arbitrary units.

or flow cytometric analysis. Serum cytokine levels were measured using the Cytokine 25-Plex Panel (Millipore; Fig. 6A, Supplemental Fig. 2). Cytokines produced by activated T cells were tested using PBMCs (2×10^5 cells per 125 μl per well). Serial dilutions of GS-9829 were preincubated with cells (60 min) before cell activation with Cytostim (anti-CD3/MHC-II, Miltenyi Biotec; 60 h), as indicated by the manufacturer. Cytokine levels in supernatants were assessed with Multiplex cytokine and chemokine kits (Meso Scale Discovery). Activated T cell supernatants (25 μl) were transferred to assay plates and developed according to manufacturer's protocols (Supplemental Fig. 3A).

Histology

Tissue samples for histology were fixed in 10% buffered formalin, embedded in paraffin, sectioned (~4 μm), and stained with H&E as described (24, 34). For immunofluorescence, fresh organs were placed in a cryoprotective embedding medium (OCT; Tissue-Tek), maintained at −80°C, sectioned (4–10 μm), blocked in PBS with 10% goat serum and 2% BSA, stained with anti-F4/80 (Rat MAb; Abcam), and incubated with FITC-conjugated goat anti-rat IgG (Pharmingen) or F4/80 (Serotec) with FITC-conjugated goat anti-rat Ab. For immunohistochemistry, sections were deparaffinized, treated with citrate buffer for Ag retrieval, blocked with an avidin/biotin blocking kit (Vector), and stained with anti-CD3 (145-2C11; Pharmingen). Biotinylated anti–CD3-stained sections were developed with streptavidin-peroxidase (Dako). Images were captured with a DP-10 digital camera on an Olympus Vanox microscope or in a Microfluor Leica SP5 microscope.

Statistics and quantitation

The Western blot signal in the linear range was quantitated with ImageJ. Data are presented as mean ± SEM. For statistics, an unpaired two-tailed Student t test (unless otherwise indicated) was used, and was ANOVA-calculated with GraphPad Prism version 5.0 software.

Results

GS-9829 is a potent and selective inhibitor of p110δ

To determine the effect of p110δ inhibition in murine systemic lupus, we first characterized the selectivity and in vivo potency of the pharmacologic p110δ inhibitor GS-9829 [(S)-2-(1-(9H-purin-6-amino-ethyl)-3-(2,6-difluorophenyl)quinazolin-4([^{3}H])-1] (Fig. 1A), a close structural analog of GS-1101 (idelalisib) (44), GS-9820 (45) and IC87114 (46), because they all derive from the same quinazolinone core structure. GS-9829 was characterized using a FRET-based in vitro kinase assay that measures PIP_3 production (detailed in *Materials and Methods*). This assay showed that GS-9829 was selective for p110δ relative to other PI3K class I enzymes (IC_{50}: p110α > 10 μM; p110β > 10 μM; p110γ > 10 μM; p110δ = 70.3 nM) and was $>10^3$-fold more selective against p110δ than against other related kinases such as CIIα, hVPS34, DNAPK, and the mammalian target of rapamycin (Fig. 1A, Table I).

Isoform potency and selectivity was also determined using a cell-based assay, as described (40). In fibroblasts, the PDGF receptor activates primarily p110α and the LPA receptor activates predominantly p110β (47, 48). In basophils, FcεRI activates p110δ and fMLP activates p110γ; activation of FcεRI and fMLP receptors induce CD63 expression (30, 49). GS-9829 reduced PDGF or LPA-induced Akt phosphorylation by <50% at 10 μM, the highest concentration tested (Fig. 1A, Table II). GS-9829 suppressed FcεRI p110δ-mediated CD63 expression with an EC_{50} of 78 nM. In contrast, fMLP p110γ-mediated CD63 expression was inhibited by <50% at 10 μM (Fig. 1A, Table II), confirming its potency and selectivity for p110δ in cells.

Although GS-9829 selectivity for the p110δ Class I PI3K isoform was shown by IC50 determinations, we tested GS-9829 binding to kinases outside the PI3K family. A high GS-9829 concentration (10 μM) in a KinomeScan assay (36) was used. GS-9829 only binds class I PI3K (Supplemental Fig. 1, Supplemental Table I) and inhibits p110δ at an IC_{50} of ~70 nM.

We administered GS-9829 dissolved in peanut oil (30 mg/kg) by oral administration to MRL/*lpr* mice. Pharmacokinetic analysis showed maximal serum concentration 4 h after administration (Fig. 1B). p110δ inhibition in vivo led to a reproducible reduction in p-Akt levels of ~50% in GS-9829–treated mouse splenocyte extracts. This reduction was detectable 12 h after GS-9829 administration (Fig. 1C), suggesting that GS-9829 can be administered in vivo (twice daily).

Table I. GS-9829 inhibitory potency (IC_{50} value) and selectivity

Class I PI3K				Class II	Class III	Related Kinases			
p110α	p110β	p110γ	p110δ	CIIα	hVPS34	PIK5α	PIK5β	DNAPK	mTOR
$>10^4$	$>10^4$	$>10^4$	70.3	$>10^4$	$>10^4$	$>10^4$	$>10^4$	$>10^5$	$>10^5$
$n = 5$	$n = 5$	$n = 5$	$n = 14$	$n = 1$	$n = 1$	$n = 1$	$n = 1$	$n = 3$	$n = 3$

The inhibitory potency (IC_{50} value) and selectivity of GS-9829 was tested using purified enzymes in a TR-FRET assay that monitors PIP_3 production. Data were normalized based on positive (DMSO) and negative (1μM wortmannin) controls. IC_{50} values were calculated from the dose-response curves. All values shown are IC_{50} (nM).

Table II. GS-9829 acts selectivity in p110δ in the cell-based assays

PI3K Isoforms	p110α	p110β	p110γ	p110δ
Cell Type	Primary Fibroblasts	Primary Fibroblasts	Human Basophils	Human Basophils
Stimulus	PDGF-induced pAkt	LPA-induced pAkt	fMLP-induced CD63	FcγRI-induced CD63
EC_{50} (nM)	$>10^4$ $n = 3$	$>10^4$ $n = 3$	$>10^4$ $n = 3$	78.0 $n = 6$

To examine the action of GS-9829 in p110α, β, δ, and γ in cell-based assays, murine embryonic fibroblasts (MEFs) for p110α and p110β were used. MEFs were stimulated for 15 min with PDGF (10 ng/ml for p110α) or with LPA (10 μM for p110β) with or without increasing concentrations of GS-9829. After stimulation, MEF were lysed and lysates examined with Western blot using pAkt and Akt Ab. For the analysis of p110δ and p110γ, basophil activation was measured in isolated PBMCs. Cells were activated with anti-FcεRI Ab (for p110δ) or with *N*-formyl-methionyl-leucyl-phenylalanine (200 nM for p110γ) in the absence or presence of increasing concentrations of GS-9829. To monitor the basophil activation, we examined CD63 and CCR3 expression. The dose-response curves to GS-9829 were used to estimate the IC_{50} (nM) of GS-9829 for each isoform. All values shown are IC_{50} (nM).

p110δ inhibition diminish lupus disease in MRL/lpr mice

To determine whether selective p110δ inhibition reduces lupus-like disease in MRL/*lpr* mice, we treated a group of mice with GS-9829 twice daily (every 12 h). Treatment began at 3 or 3.5 months old, the period in which most untreated MRL/*lpr* mice show the first signs of kidney disease (as determined by proteinuria; Fig. 2A). Treatment was terminated at ~5.5 mo, when half of the control mice (vehicle-treated) showed signs of discomfort because of renal disease. GS-9829 administration reduced proteinuria (Fig. 2A).

Histologic examination of the kidney at experiment termination (~5.5 mo) showed that whereas control MRL/*lpr* mice had severe mesangioproliferative glomerulonephritis (GN) with scores of 4–6 based on International Society of Nephrology–Renal Pathology Society criteria (50), the GN score for GS-9829–treated mice was lower (0–2; Fig. 2B, 2C). The experiment initiated at 3.5 mo showed that GS-9829 treatment induced a moderate improvement, even when treatment began after the appearance of disease symptoms (~3 mo).

Glomerulonephritis in lupus-prone mice is caused by the combined action of local inflammation and deposition of Ig complexes (12–15). We examined immunocomplex accumulation and kidney infiltration by inflammatory cells in control and GS-9829–treated mice. Treated mice showed less immunocomplex deposition and lower serum anti-dsDNA Ab levels (Fig. 3A, 3B). Moreover, mice treated beginning at 3 or 3.5 mo had a longer lifespan, indicating clinical improvement by p110δ inhibition even after the appearance of proteinuria (at ~3 mo; Fig. 3C). The results show that p110δ inhibition reduces the severity of systemic lupus-like disease in the mouse.

We evaluated T cell and macrophage infiltration into the kidney. There were no significant differences in T cell infiltration between control and treated MRL/*lpr* mice. In contrast, treated mice showed more than 50% reduction in macrophage infiltration (Fig. 3D, 3E). We also tested whether GS-9829 administration induced undesired side effects such as weight loss or altered glucose levels. Mice were weighed every 5 d, and blood glucose levels were measured every 15 d. There were no significant differences in these parameters between GS-9829–treated and control mice (Fig. 3F).

Effect of p110δ inhibition on lymphocyte populations in lupus-prone mice

MRL/*lpr* mice show marked enlargement of spleen and lymph nodes because of the accumulation of hematopoietic cells, including T and B lymphocytes (37). We analyzed hematopoietic cell populations in control and treated mouse spleens. GS-9829 treatment reduced spleen weight and the absolute number of mononuclear cells (Fig. 4A, Supplemental Fig. 2A). The numbers of B ($B220^+CD3^-$) and T ($B220^-CD3^+$) cells tended to be lower in treated mice, as was also the case for $CD4^+$ T cells (Fig. 4B, 4C). The $CD4^-CD8^-CD3^+B220^+$ lymphocyte population present in human and murine lupus (30) was significantly reduced by

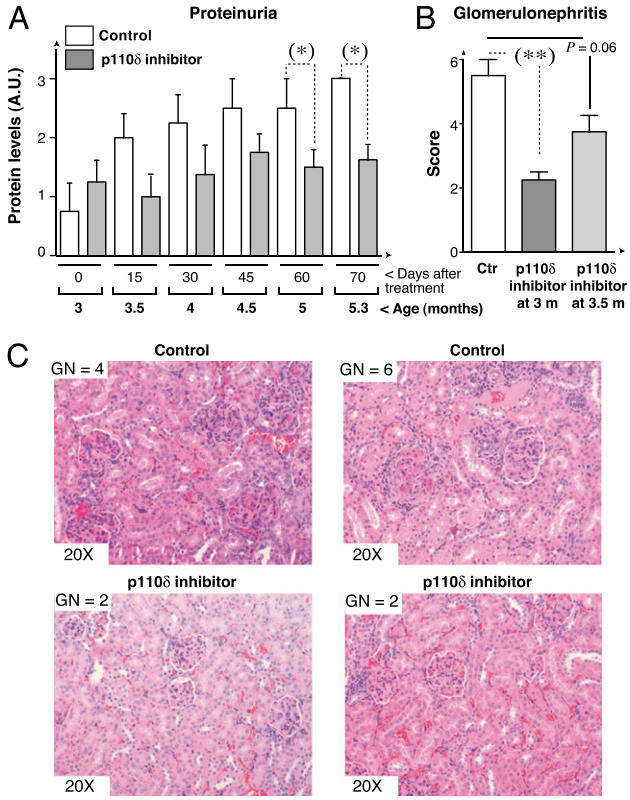

FIGURE 2. p110δ inhibition reduced glomerulonephritis in MRL/*lpr* mice. (**A**) MRL/*lpr* mice (3 mo old) were treated every 12 h with GS-9829 (30 mg/kg) for 70 d. Protein concentration in urine was measured every 15 d. The graph shows proteinuria levels (mean ± SD; $n = 12$). (**B** and **C**) MRL/*lpr* mice were treated orally every 12 h with GS-9829 (30 mg/kg) from age 3 or 3.5 mo until ~5.5 mo, when they were sacrificed and kidney sections were stained with H&E. The graph (B) shows the mean ± SD glomerulonephritis (GN) International Society of Nephrology–Renal Pathology Society score (ranking from 0 to 6) in controls and GS-9829–treated mice ($n = 12$, each). Images (C) show representative sections from control or GS-9829-treated MRL/*lpr* mice. GN score is indicated. Original magnification ×20. *$p < 0.05$, Student *t* test. A.U., arbitrary units.

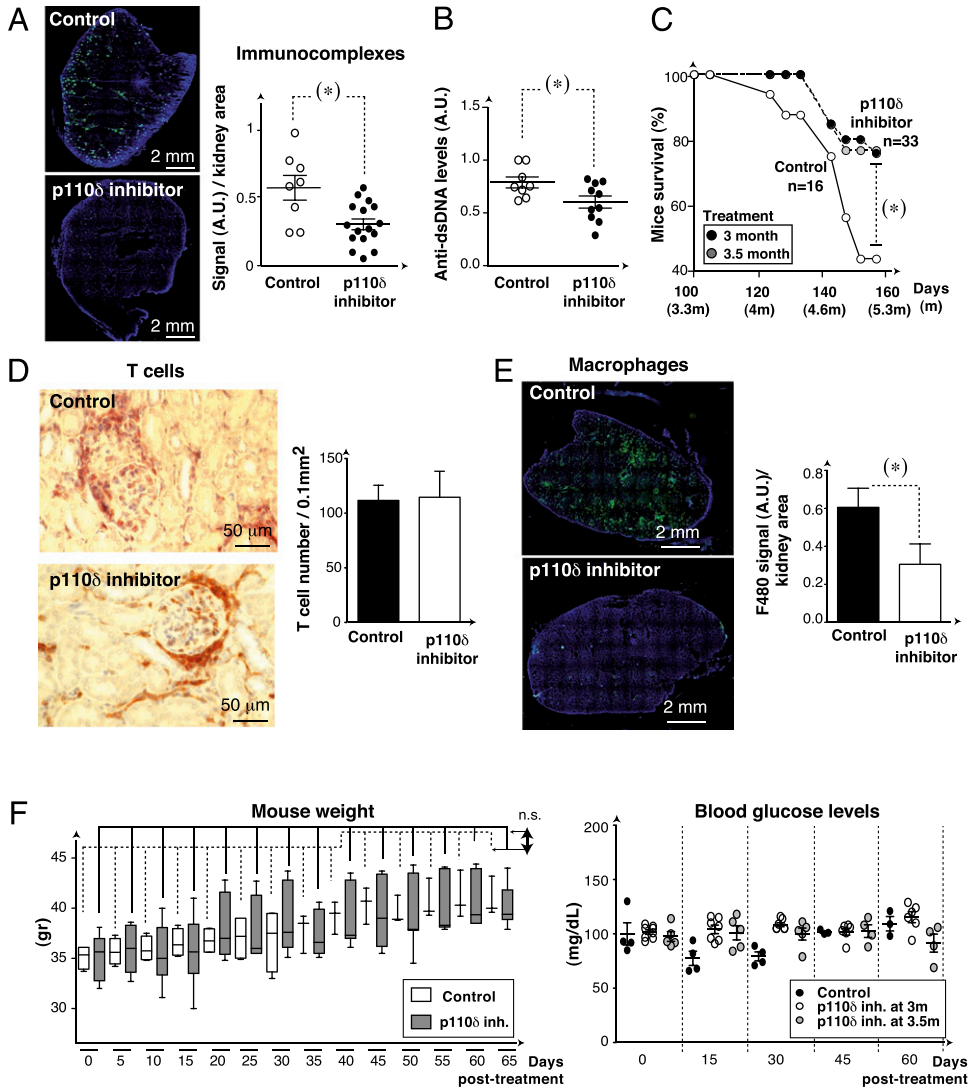

FIGURE 3. Prolonged life span and reduced kidney damage in MRL/*lpr* mice treated with p110δ pharmacologic inhibitors. (**A**) MRL/*lpr* mice were treated orally every 12 h with GS-9829 (30 mg/kg) from 3 to 5.5 mo of age, at which time they were sacrificed. The images show a representative kidney section from a control and a GS-9829–treated MRL/*lpr* mouse, stained with anti-mouse IgG Ab. The graph shows IgG signal intensity normalized for kidney area in each section and relative to 1 (maximal; mean ± SD). *$p < 0.01$, Student *t* test. (**B**) MRL/*lpr* mice were treated as in (A). Serum anti–double strand (ds)-DNA Ab levels (A.U.) were measured by ELISA ($n = 10$; mean ± SD). *$p < 0.05$, Student *t* test. (**C**) Mouse survival (percent) at various times after GS-9829 treatment. MRL/*lpr* mice were treated with vehicle (control) or GS-9829 (30 mg/kg) starting at month 3 ($n = 20$) or 3.5 ($n = 13$). *$p < 0.05$, log-rank Mantel-Cox test. (**D** and **E**) Kidney sections from MRL/*lpr* mice treated as in (A) were examined by immunohistochemistry using CD3 Ab (D) or F4/80 MAb, which recognizes macrophages (E). Images show representative sections from control or treated MRL/*lpr* mice. Graphs show the number of T cells (mean ± SD; $n = 12$) in a 0.1 mm^2 area (D) or normalized F4/80 signal intensity (examined as in A; $n = 12$) (E). (**F**) MRL/*lpr* mice were treated as in (A). The graph (*left panel*) shows mouse weight as measured every 5 d (mean ± SD; $n = 12$). Blood glucose levels (*right panel*) in control or GS-9829–treated animals ($n = 4$ per group). n.s., not significant (ANOVA).

p110δ inhibition. $CD11b^+$ numbers, which include macrophages and neutrophils, were not affected (Fig. 4C).

We analyzed memory T cells because they include autoreactive T lymphocytes (6–8). Naive lymphocyte numbers were low in MRL/*lpr* mice, as reported previously (24). p110δ inhibition led to a significant reduction in the percentage and numbers of $CD4^+$ effector memory cells ($CD44^{high}CD62L^{low}$) and a tendency to increased percentages of naive ($CD44^{low}CD62L^{low}$) and central memory ($CD44^{high}CD62L^{high}$) cells (Fig. 5A, Supplemental Fig. 2B). MRL/*lpr* mice have fewer $CD8^+$ than $CD4^+$ effector memory cells. $CD8^+$ effector memory cells were unaffected by GS-9829 treatment (Fig. 5A). Tregs and Th17 cells have both been implicated in the pathogenesis of autoimmune disease (51, 52). p110δ regulates Treg differentiation (53); accordingly, p110δ inhibition reduced Treg numbers and the proportion of Th17 $CD4^+$ T cells (Fig. 5B, 5C). These analyses showed that p110δ inhibition in MRL/*lpr* mice tends to reduce total B and T cell numbers as well as the percentages of $CD4^+IL\text{-}17^+$, $CD4^-CD8^-CD3^+B220^+$, $CD4^+$ effector memory, and Tregs.

More than 50% of human SLE patients show enhanced p110δ activation in T cells and defective activation-induced cell death (AICD) (36). p110δ inhibition corrected the AICD defect of SLE patient T cells in vitro (36), suggesting that p110δ enhances activated and/or memory T cell survival and promotes T and B cell accumulation in SLE. AICD cannot be studied in MRL/*lpr* mice because Fas is mutated in this mouse strain (*lpr* mutation) (37). Nonetheless, given that $CD4^-CD8^-CD3^+B220^+$ cells, autoantibody-producing B cells and $CD4^+$ memory cells were reduced by p110δ inhibition (Figs. 4, 5A), we hypothesized that p110δ could regulate cell survival in the MRL/*lpr* mouse via a different cell death receptor.

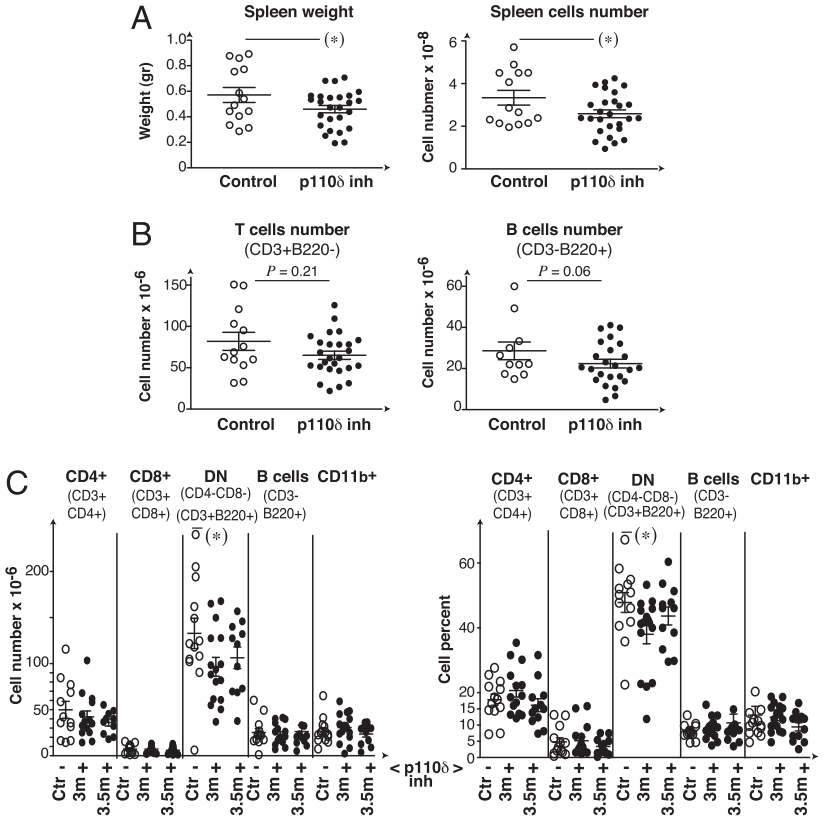

FIGURE 4. p110δ inhibition reduces B and T lymphocyte numbers in MRL/*lpr* mice. (**A**) MRL/*lpr* mice were treated orally every 12 h with GS-9829 (30 mg/kg) from 3 or 3.5 mo of age until ~5.5 mo of age, at which time they were sacrificed. Spleen weight and cell numbers are shown. (**B** and **C**) Mice were treated as in (A). Graphs show cell number or percentage of B and T cells (B) or indicated populations (C). $*p < 0.05$, Student *t* test.

PI3K regulates NF-κB transcription factor activity, which in turn controls expression of the prosurvival factor Bcl-xL (54, 55). We tested whether levels of Bcl-xL, which regulate activated B and T cell survival (56, 57), were affected by GS-9829 treatment in splenocytes collected at experiment termination. As a control, we analyzed p-Akt levels. We found a marked decrease in p-PKB and Bcl-xL levels in GS-9829–treated MRL/*lpr* mouse cells compared with controls (Fig. 5D). The reduction in Bcl-xL levels likely mediates the reduction in the number of autoreactive B and T cells (the latter included in the $CD4^+$ effector memory T cell population) in GS-9829–treated mice.

*Altered cytokine production in GS-9829–treated MRL/*lpr *mice*

We tested whether p110δ inhibition altered serum levels of representative cytokines and chemokines. Most were found at very low levels in serum (such as GM-CSF, IFN-γ, IL-1α, IL-1β, IL-2, IL-17). Another group showed higher levels that did not vary after GS-9829 treatment (e.g., IL-10, G-CSF, IP-10, MIP1α; Supplemental Fig. 2C). In contrast, IL-6 and TNF-α were at high levels in MRL/*lpr* mice and decreased after GS-9829 treatment (Fig. 6A).

Serum cytokine levels are also low in healthy mice, but can be examined after T cell activation in vitro. Compared with controls, activated p110δ-deficient T cells show lower levels of Th1 cytokines (e.g., IFN-γ). Similarly, TCR-activated PBMCs treated with a p110δ inhibitor show decreased Th1 cytokine levels (58). We determined the GS-9829 dose needed to inhibit production of various cytokines in activated PBMCs; TNF-α and IL-17 were the most sensitive cytokines, but IL-12, IL-4, and IL-13, and to a lesser extent IL-10 and IL-5 were also inhibited at nanomolar GS-9829 concentrations (Supplemental Fig. 3A).

To study Th1/Th2 cell polarity further, we measured the levels of IgG isotypes produced in these mice. All IgG tended to be reduced in GS-9829–treated mice, with a significant decrease in the Th1-linked isotype IgG2b (Fig. 6B). Although both Th1 and Th2 cytokines tended to be reduced by GS-9829 treatment in MRL/*lpr* mice, Ab production and the reduction in proinflammatory cytokines IL-6 and TNF-α after treatment indicate a more marked inhibition of Th1 than of Th2 polarity in these mice.

p110δ regulates macrophage ability to cross the basement membrane

An unpredicted effect of p110δ inhibition in MRL/*lpr* mice was the apparent decrease in kidney macrophage infiltration (Fig. 3E), which is not observed after pharmacologic inhibition of the other hematopoietic isoform, p110γ (34). The effect of GS-9829 treatment in reducing TNF-α levels could alter macrophage infiltration, as TNF-α regulates vascular permeability (59, 60). In addition, p110δ inhibition might affect intrinsic macrophage capacity to cross basement membranes and infiltrate the kidney.

We isolated native basement membrane from wild type mice and derived macrophages from the bone marrow of mice that express an inactive form of p110δ ($p110\delta^{D910A/D910A}$; [$p110\delta^{DA/DA}$]). As controls, we derived macrophages from wild type and p110γ-deficient mice (31). BMDM numbers generated from $p110\gamma^{-/-}$ and $p110\delta^{DA/DA}$ mice were slightly lower than those from wild type littermates, although the difference was not significant (Fig. 7A). BMDM from these mice did not differ in phenotypic markers ($CD11b^+$ and $F4/80^+$) from their wild type littermates (Fig. 7A). Compared with control or p110γ-deficient macrophages, $p110\delta^{DA/DA}$-expressing macrophages showed a reduced capacity to cross the basement membrane and degrade collagen IV (Fig. 7B, 7C).

We also compared basement membrane invasion of BMDMs treated with isoform-specific p110δ (GS-9829, 0.2 μM) or p110γ inhibitor (AS-605240, 1 μM; Ref. 43). We used a dose sufficient to inhibit p110 in cultured cells but that did not induce cell death after 3 d in culture (Supplemental Fig. 3B). A slightly cytotoxic effect was observed only when inhibitors were used at 10 μM (Supplemental Fig. 3B). We assessed macrophage invasion on

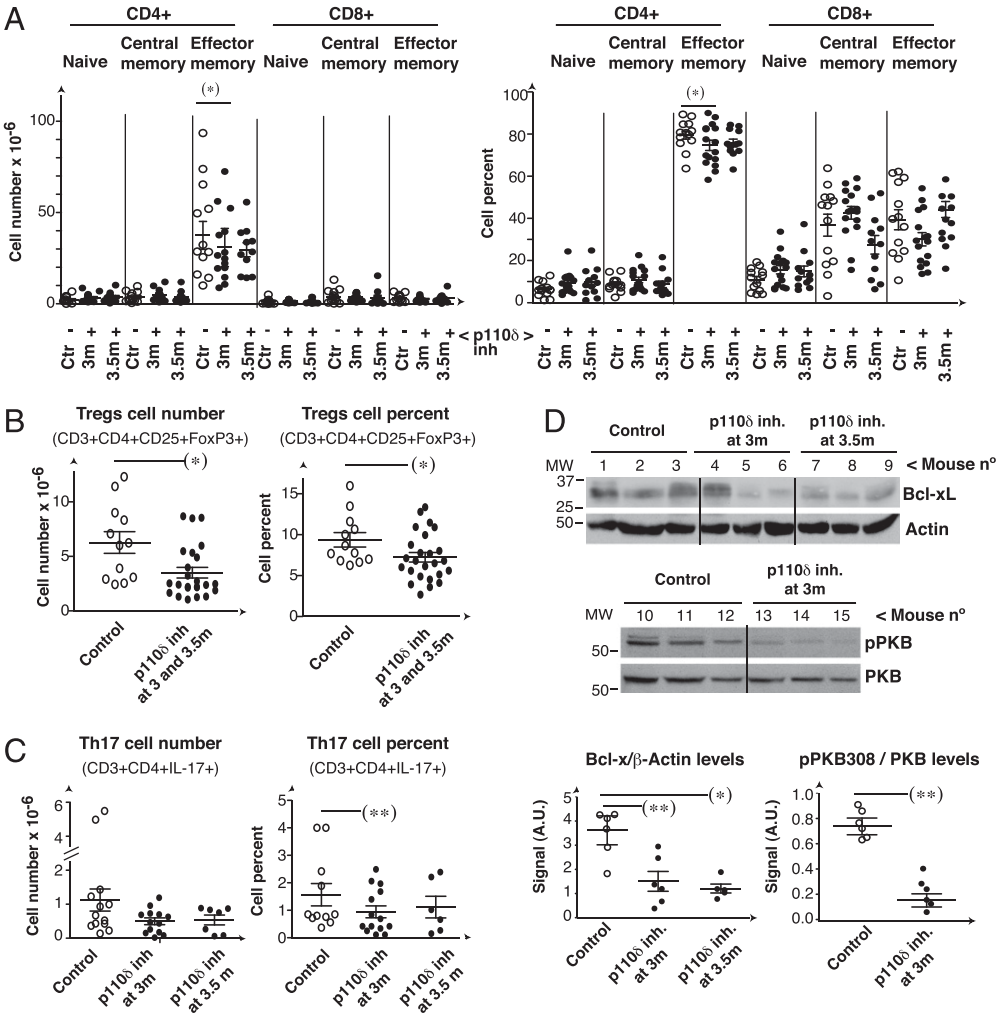

FIGURE 5. p110δ inhibition reduces CD4$^+$ effector memory cells in MRL/*lpr* mice. (**A**) MRL/*lpr* mice were treated orally every 12 h with GS-9829 (30 mg/kg) from age 3 or 3.5 mo to age 5.5 mo, at which time they were sacrificed. Percentage and total number of CD4$^+$ or CD8$^+$ T cells with naive (CD44^{low} CD62L^{low}), effector (CD44^{high}CD62L^{low}) or central memory (CD44^{high} CD62L^{high}) phenotypes, as determined with flow cytometry. (**B** and **C**) Mice were treated as in (A). The percentage and total cell number of CD4$^+$CD25$^+$Foxp3$^+$ Tregs (B) (3 and 3.5 mo plotted together) or of CD4$^+$IL-17$^+$ T cells (C) was measured with flow cytometry. (**D**) MRL/*lpr* mice were treated orally every 12 h with GS-9829 (30 mg/kg) from month 3 or 3.5 (indicated) until ~5.3 mo, at which time they were sacrificed. Splenocyte extracts were analyzed with Western blot using the indicated Ab. The graphs show the signal in arbitrary units (A.U.) of indicated proteins normalized to the loading control. *$p < 0.05$, Student *t* test; **$p < 0.01$; *t* test in (C) was paired.

basement membranes treated with GS-9829 (0.2 μM), AS-605240 (1 μM), or DMSO as control. BMDMs treated with the PI3Kδ inhibitor GS-9829 degraded less collagen IV than did those treated with DMSO or the PI3Kγ inhibitor AS-605240 (Fig. 7D). Moreover, treatment with p110δ inhibitor led to macrophage accumulation in the upper layer of the basement membrane and fewer macrophages crossing the membrane compared with DMSO- or AS-605240-treated BMDM (Fig. 7D). These findings confirmed our observations that p110δ deficiency impaired macrophage invasion in BMDM from p110δ$^{DA/DA}$ but not from p110γ$^{-/-}$ mice. The data suggest that defective kidney infiltration after p110δ inhibition might also be caused by a direct effect on the transmigratory capacity of macrophages.

Discussion

Development of specific therapeutic approaches for SLE autoimmune disease is still an objective of basic research. Increased PI3K activation in T cells is sufficient to trigger systemic lupus in the mouse (24). Genetic inactivation of the p110γ isoform in MRL/*lpr* mice, a mammalian SLE model, reduces this disease (34). Nonetheless, p110δ is the isoform frequently activated in human SLE (36). In this study, we examined the effect of p110δ inhibition in a mouse model of systemic lupus. p110δ inhibition in MRL/*lpr* mice reduced lupus symptoms and extended life span. Analysis of the mechanism by which the p110δ inhibitor acted on MRL/*lpr* mice showed that p110δ inhibition reduced the excessive number of B and activated/memory T cells as well as serum TNF-α levels and kidney infiltration by macrophages. The decrease in TNF-α levels might affect macrophage infiltration, as TNF-α regulates vascular permeability (59, 60). In addition, p110δ inhibition impeded macrophage capacity to cross basement membranes, and could thus help to reducing the macrophage infiltrate. These results validate the use of p110δ pharmacologic inhibitors for SLE treatment.

Comparison of GS-9829 with previously described inhibitors showed comparable selectivity for p110δ (compared with p110α, p110β, and p110γ) and potency to those of AS15 and PIK-39 (61); this selectivity was maintained in cell-based assays. In the mouse, GS-9829 (oral administration at 30 mg/kg) appeared rapidly in serum and enabled 50% p-AKT inhibition in splenocytes at 12 h. GS-9829 is a close structural analog of GS-1101 (idelalisib), a selective inhibitor of p110δ currently in clinical

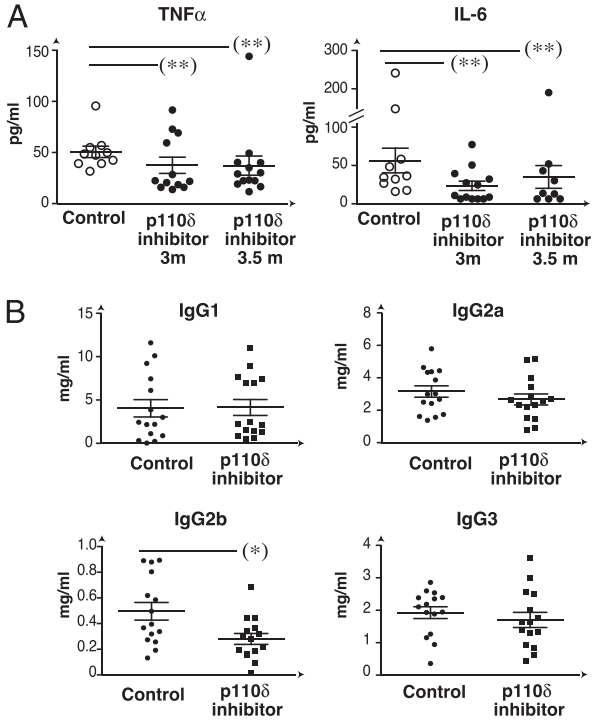

FIGURE 6. GS-9829 treatment reduced serum TNF-α and IL-6 levels in MRL/*lpr* mice. (**A**) Cumulative data for serum TNF-α and IL-6 levels in control and GS-9829–treated MRL/*lpr* mice. GS-9829 treatment started at 3 or 3.5 mo of age until ~5.5 mo of age, when they were sacrificed (30 mg/kg every 12 h). (**B**) Anti-dsDNA IgG1, IgG2a, IgG2b, and IgG3 in mice treated as in (A). Abs and cytokines were measured by ELISA. $*p < 0.05$, paired Student *t* test; $**p < 0.01$.

testing for the treatment of hematological malignancies (44). We selected GS-9829 for study in the *MRL/lpr* SLE model because it has a longer half-life in serum than GS-1101 does. Human kinome-screen assays showed that at high concentration (10 μM), GS-9829 remained selective to class I PI3K. GS-9829 treatment was well tolerated by MRL/*lpr* mice, and we observed no significant treatment-related adverse events. In addition, GS-9829 improved kidney function (as assessed by reduction in proteinuria and nephritis) and extended lifespan in MRL/*lpr* mice, providing in vivo evidence that p110δ is a potential therapeutic target for SLE. The effectiveness of GS-9829 in our murine lupus model also suggests its utility in treatment of the recently described "activated PI3Kδ syndrome" (62, 63).

Inhibition of the other hematopoietic PI3K isoform, PI3Kγ, also improves lupus symptoms in MRL/*lpr* mice (34, 35). Pharmacologic inhibition of p110δ (Fig. 4) or p110γ (34) reduced B and T cell numbers in MRL/*lpr* mice. Because p110δ regulates T and B cell survival (26, 64, 65), this might explain the reduction in lymphocyte numbers following GS-9829 treatment. $CD4^-CD8^-CD3^+B220^+$ cells increase markedly in murine lupus and are found in kidneys of lupus nephritis patients, indicating a contribution to kidney damage (51). These cells were also reduced by p110δ (Fig. 4) or p110γ inhibitors (34). $CD4^+$ effector memory cell numbers were also decreased by GS-9829 and p110γ inhibitors in MRL/*lpr* mice (Fig. 5) (34–36); at least in the mouse, PI3Kγ therefore cooperates with PI3Kδ for memory cell survival. In contrast, PI3Kδ inhibition, but not that of PI3Kγ, reduced kidney-infiltrating macrophages. Although PI3Kγ contributes to murine lupus, only the PI3Kδ isoform is frequently activated in human SLE (36), supporting that PI3Kδ is a more appropriate target for human SLE.

Treg and Th17 cell numbers were also reduced in GS-9829-treated MRL/*lpr* mice. These populations have not been examined in PI3Kγ inhibitor-treated MRL/*lpr* mice (34, 35), although the observation that differentiation of these cells requires PI3Kγ and PI3Kδ activity (53, 66, 67) suggests that both isoforms control these cell types. Although Tregs are needed to counteract autoreactive T cells, the decrease in the $CD4^+Foxp3^+$ population in GS-9829–treated MRL/*lpr* mice might be beneficial, as in human SLE there is a $CD4^+Foxp3^+$ T cell population functionally defective for effector cell inhibition and for production of proinflammatory cytokines such as IL-17 (68). $CD4^-CD8^-CD3^+B220^+$ cell population also contributes to the pathogenesis of kidney damage in lupus (51). The smaller number of Th17 T cells and of $CD4^-CD8^-CD3^+B220^+$ cells, which also produce IL-17 (69), could help to alleviate lupus in MRL/*lpr* mice after GS-9829− treatment.

Analysis of the effect of PI3Kδ inhibition on autoantibody and cytokine production in MRL/*lpr* mice showed that all IgG isotypes were moderately decreased in serum, with a greater reduction in the Th1-IgG2b isotype. Most Th1 and Th2 cytokines were barely detectable in serum; nonetheless, in vitro stimulation of T cells showed that GS-9829 treatment reduced Th1 and Th2 cytokines. A similar assay using T cells from inactive PI3Kγ or inactive PI3Kδ transgenic mice shows a modest PI3Kγ contribution to Th1 and Th2 cell differentiation, and a more marked role for PI3Kδ in Th cell differentiation (66, 67). These observations suggest that PI3Kδ and PI3Kγ have a partially redundant function in helper cell differentiation (Th1 and Th2), with a greater contribution by PI3Kδ. The most notable effect of GS-9829 treatment in MRL/*lpr* mouse cytokines was the reduction in IL-6 and TNF-α.

TNF-α is a pleiotropic inflammatory cytokine with a critical function in acute phase responses; it is produced mainly by macrophages, T lymphocytes, and kidney-resident cells (in lupus) (59, 70). TNF-α is necessary for pathogen clearance (71), but excess TNF-α production mediates the uncontrolled immune response observed in fatal septic shock (70). TNF-α initiates a cytokine cascade that increases vascular permeability, thereby regulating macrophage recruitment to different organs; TNF-α levels are increased in lupus patients (59, 60). As TNF-α regulates macrophage infiltration to kidney, it is likely that defective TNF-α production helps to reduce this infiltrate after PI3Kδ inhibition. IL-6 is secreted by T cells and macrophages, induced during the physiologic immune response, and increased in SLE patients (72). Reduction of TNF-α and IL-6 levels by PI3Kδ inhibitors appears to be isoform-specific. Although the effect of PI3Kγ inhibition on these cytokines in MRL/*lpr* mice has not been studied, inhibition of PI3Kδ but not of PI3Kγ decreases TNF-α production in T cells from healthy mice (73). TNF-α and IL-6 involvement in kidney damage in lupus (59, 60, 72) suggests that GS-9829 reduction of their levels help to mitigate disease in MRL/*lpr* mice.

We report that p110δ inhibition reduced kidney infiltration by macrophages (Fig. 3). Previous studies examined the effect of impaired PI3Kδ activity in murine lupus. Winkler et al. (74) described a dual PI3Kδ/PI3Kγ inhibitor (IPI-145) that blocks the adaptive and innate immune responses by inhibiting B and T cell proliferation, neutrophil migration, and basophil activation. They explored IPI-145 activity in collagen-induced arthritis, OVA-induced asthma, and SLE; IPI-145 showed potent activity in all these systems. In lupus, IPI-145 (1 mg/kg) reduced glomerulonephritis in NZBWF1/J mice, but had no effect on dsDNA autoantibody levels, although PI3Kδ was inhibited (74). Our results are in agreement with their findings on the therapeutic action of PI3Kδ inhibition in a distinct lupus model, although they did not test the action of the dual inhibitor on macrophages. Maxwell

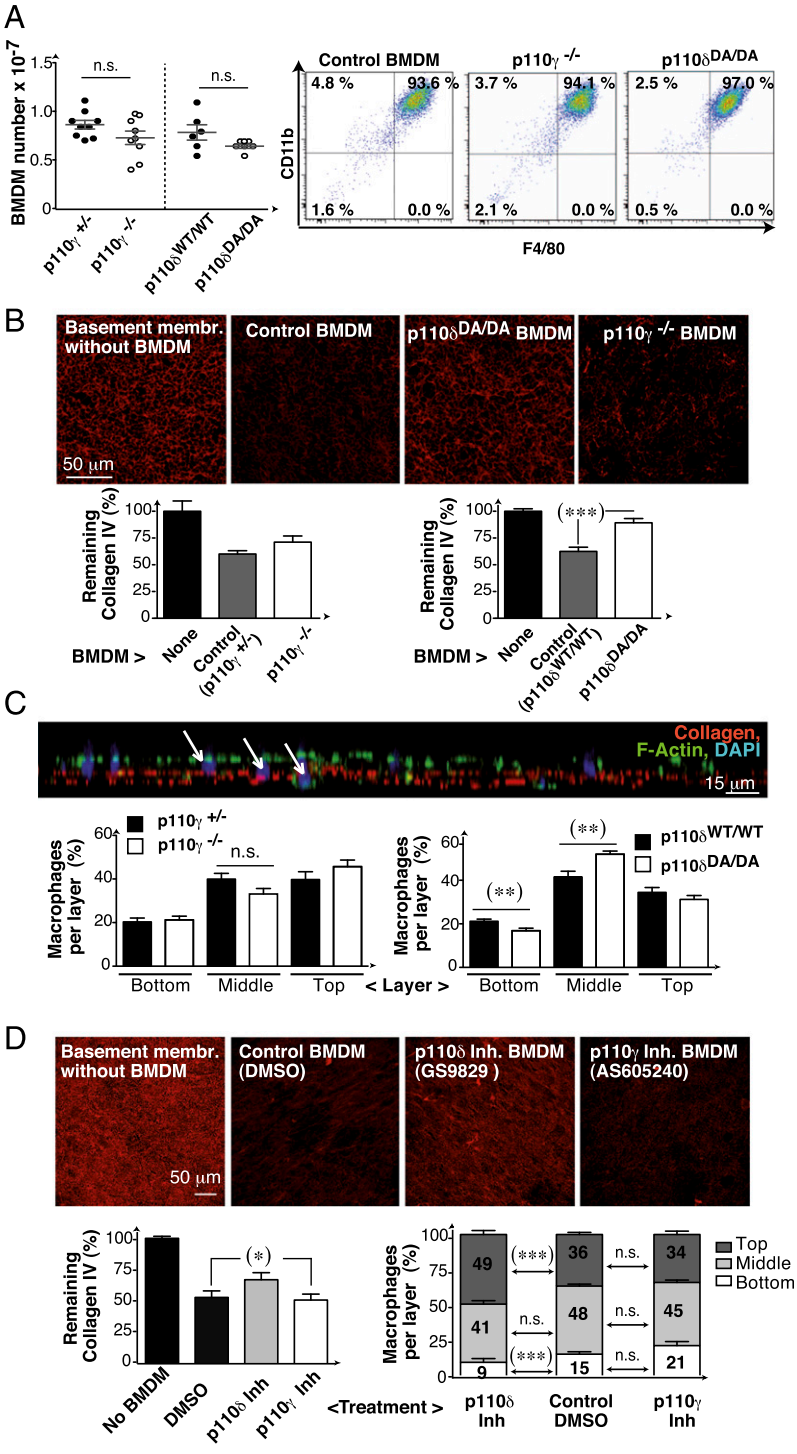

FIGURE 7. p110δ inactivation impairs BMDM basement membrane degradation. (**A**) BMDM were generated from p110γ$^{-/-}$, p110δ$^{DA/DA}$ mice, and control littermates (see *Materials and Methods*). The graph shows BMDM numbers from the different mice (mean ± SD; $n = 6$; two-tail Wilcoxon matched-pairs sign rank test). CD11b^{+} and F4/80^{+} expression in BMDM was examined with flow cytometry using appropriate Ab. (**B**) BMDMs generated as in (A) were seeded onto basement membrane from wild type mice. After 3 d in culture alone or with the indicated BMDM, basement membrane collagen IV was stained by immunofluorescence, and the signal in a similar area was quantitated using ImageJ for the different conditions. Data are presented as the remaining collagen IV signal in basement membranes cultured with different BMDMs compared with control membranes (considered 100%; mean ± SEM; $n = 4$). (**C**) BMDMs were seeded on basement membranes from wild type mice as in (A) for 72 h. Basement membrane invasion was analyzed by immunofluorescence staining of BMDM (F-actin with phalloidin-A488 and nuclei with DAPI) and of basement membrane (collagen IV, red). The graph shows the proportion of BMDMs in each layer compared with total BMDMs in the different layers examined in different z-sections (100%; mean ± SEM; $n = 3$). (**D**) BMDMs from C57BL/6J mice were seeded onto basement membrane as in (A) and treated with GS-9829 (0.2 μM) or AS-605240 (1 μM) every 12 h. BMDM invasion was examined as in (B) and (C). Remaining collagen (*left panel*) was as in (B), and the percentage of BMDMs in the different layers is relative to total (100%; mean ± SEM; $n = 3$; *right panel*). Student *t* test (two-tailed Mann–Whitney test), $*p < 0.05$, $**p < 0.01$, $***p < 0.001$. n.s., not significant.

et al. (75) also studied the effect of heterozygous PI3Kδ inactivation in Lyn-deficient lupus-prone mice, which showed decreased autoantibody levels and kidney damage. B cell signaling was unaltered by heterozygous PI3Kδ inactivation, but IgG titers and T cell activation were markedly reduced, indicating a contribution of T cell inhibition in disease amelioration (75), in accordance with our study. PI3Kδ inhibition in BXSB mice also reduces autoantibody levels and proteinuria and improves survival (76); the authors found reduced pAKT and MCP-1 levels in kidney, which might contribute to the reduction in kidney-infiltrating macrophages described here.

p110δ action on kidney infiltration by macrophages (Fig. 3) has not been observed after pharmacologic inhibition of p110γ (34). We show that, in addition to reducing TNFα and presumably TNF-α–mediated macrophage recruitment to the kidney (59, 60), p110δ inactivation attenuated macrophage transmigration. To infiltrate the kidney, macrophages must cross the blood vessel and kidney basement membranes. We derived macrophages from bone marrow of mice expressing an inactive p110δ form (p110δ$^{DA/DA}$), wild type, or p110γ-deficient mice, and we analyzed their ability to cross native basement membrane purified from syngeneic wild type mice. Whereas M-CSF–induced macrophage differentiation was not significantly affected by p110δ inactivation or p110γ deletion, the ability of macrophages from p110δ$^{DA/DA}$ mice to cross the basement membrane and degrade collagen IV was reduced compared with p110γ-deficient or control mice. Results

were similar when we tested the effect of p110γ and p110δ inhibition. These observations suggest that p110δ inhibition induces a reduction in TNFα levels and in macrophage transmigration capacity, which might explain the reduction in kidney infiltration by macrophages. Macrophage infiltrates contribute to lupus nephritis (16–18, 77, 78), suggesting that the therapeutic action of GS-9829 treatment involves reduction of this infiltrate. Although irrelevant in macrophage infiltration of the kidney in our system, p110γ regulates macrophage chemotaxis toward RANTES MIP-5, MDC, SDF-1, as well as C5a and is necessary for peritoneal recruitment of macrophages in a septic shock model (31).

We show that treatment of the MRL/*lpr* SLE mouse model with a p110δ inhibitory compound extended lifespan and reduced kidney damage, even when administered after appearance of disease symptoms (~3 mo). GS-9829 treatment had no apparent secondary effects. Restoration of renal function is important, because kidney failure remains the main cause of death in patients with SLE (79). p110δ inhibition in lupus-prone mice reduced several pathogenic cell populations, including B cells, Th17, and effector memory $CD4^+$ T cells. In addition, GS-9829 treatment decreased TNF-α and IL-6 cytokine levels as well as macrophage transmigration capacity, thereby reducing the macrophage infiltrate in the kidney, which contributes to kidney dysfunction. These observations validate that PI3Kδ is a promising therapeutic approach in SLE.

Acknowledgments

We thank the CNB Confocal Service for basement membrane assay image processing, L. Lad for assistance with PI3K biochemical assays, A. Kashishian for fibroblast assays, J. Treiberg and J. Evarts for GS-9829 synthesis, I. Lepist for PK analysis, C. Queva for helpful comments on the manuscript, E. Hirsch and J.M. Penninger for p110γ-deficient mice, B. Vanhaesebroeck for $p110\delta^{DA/\ DA}$ mice, and C. Mark for editorial assistance.

Disclosures

K.D.P. and B.H.S. are employees of Gilead Sciences, the manufacturer of GS-9829.

References

1. Graham, R. R., S. V. Kozyrev, E. C. Baechler, M. V. Reddy, R. M. Plenge, J. W. Bauer, W. A. Ortmann, T. Koeuth, M. F. González-Escribano, B. Pons-Estel, et al. 2006. A common haplotype of interferon regulatory factor 5 (IRF5) regulates splicing and expression and is associated with increased risk of SLE. *Nat. Genet.* 38: 550–555.
2. Lang, T. J., P. Nguyen, J. C. Papadimitriou, and C. S. Via. 2003. Increased severity of murine lupus in female mice is due to enhanced expansion of pathogenic T cells. *J. Immunol.* 171: 5795–5801.
3. Borchers, A. T., S. M. Naguwa, Y. Shoenfeld, and M. E. Gershwin. 2010. The geoepidemiology of systemic lupus erythematosus. *Autoimmun. Rev.* 9: A277–A287.
4. Wentworth, J., and C. Davies. 2009. Systemic lupus erythematosus. *Nat. Rev. Drug Discov.* 8: 103–104.
5. Chatham, W. W., and R. P. Kimberly. 2001. Treatment of lupus with corticosteroids. *Lupus* 10: 140–147.
6. Han, B. K., A. M. White, K. H. Dao, D. R. Karp, E. K. Wakeland, and L. S. Davis. 2005. Increased prevalence of activated CD70+CD4+ T cells in the periphery of patients with systemic lupus erythematosus. *Lupus* 14: 598–606.
7. Vratsanos, G. S., S. Jung, Y. M. Park, and J. Craft. 2001. CD4(+) T cells from lupus-prone mice are hyperresponsive to T cell receptor engagement with low and high affinity peptide antigens: a model to explain spontaneous T cell activation in lupus. *J. Exp. Med.* 193: 329–337.
8. Golan, T. D., K. B. Elkon, A. E. Gharavi, and J. G. Krueger. 1992. Enhanced membrane binding of autoantibodies to cultured keratinocytes of SLE patients after ultraviolet B/ultraviolet A irradiation. *J. Clin. Invest.* 90: 1067–1076.
9. Inghirami, G., J. Simon, J. E. Balow, and G. C. Tsokos. 1988. Activated T lymphocytes in the peripheral blood of patients with systemic lupus erythematosus induce B cells to produce immunoglobulin. *Clin. Exp. Rheumatol.* 6: 269–276.
10. Shlomchik, M. J., J. E. Craft, and M. J. Mamula. 2001. From T to B and back again: positive feedback in systemic autoimmune disease. *Nat. Rev. Immunol.* 1: 147–153.
11. D'Cruz, D. P., M. A. Khamashta, and G. R. V. Hughes. 2007. Systemic lupus erythematosus. *Lancet* 369: 587–596.
12. Kuroiwa, T., and E. G. Lee. 1998. Cellular interactions in the pathogenesis of lupus nephritis: the role of T cells and macrophages in the amplification of the inflammatory process in the kidney. *Lupus* 7: 597–603.
13. Klinman, D. M., and A. D. Steinberg. 1995. Inquiry into murine and human lupus. *Immunol. Rev.* 144: 157–193.
14. Dai, C., Z. Liu, H. Zhou, and L. Li. 2001. Monocyte chemoattractant protein-1 expression in renal tissue is associated with monocyte recruitment and tubulointerstitial lesions in patients with lupus nephritis. *Chin. Med. J. (Engl.)* 114: 864–868.
15. Hoffman, R. W. 2004. T cells in the pathogenesis of SLE. *Clin. Immunol.* 113: 4–13.
16. Tesch, G. H., S. Maifert, A. Schwarting, B. J. Rollins, and V. R. Kelley. 1999. Monocyte chemoattractant protein 1-dependent leukocytic infiltrates are responsible for autoimmune disease in MRL-Fas(lpr) mice. *J. Exp. Med.* 190: 1813–1824.
17. Lenda, D. M., E. R. Stanley, and V. R. Kelley. 2004. Negative role of colony-stimulating factor-1 in macrophage, T cell, and B cell mediated autoimmune disease in MRL-Fas(lpr) mice. *J. Immunol.* 173: 4744–4754.
18. Wang, Y., and D. C. Harris. 2011. Macrophages in renal disease. *J. Am. Soc. Nephrol.* 22: 21–27.
19. Delgado-Vega, A., E. Sánchez, S. Löfgren, C. Castillejo-López, and M. E. Alarcón-Riquelme. 2010. Recent findings on genetics of systemic autoimmune diseases. *Curr. Opin. Immunol.* 22: 698–705.
20. Krishnan, S., V. G. Warke, M. P. Nambiar, G. C. Tsokos, and D. L. Farber. 2003. The FcR gamma subunit and Syk kinase replace the CD3 zeta-chain and ZAP-70 kinase in the TCR signaling complex of human effector CD4 T cells. *J. Immunol.* 170: 4189–4195.
21. Kong, P. L., J. M. Odegard, F. Bouzahzah, J. Y. Choi, L. D. Eardley, C. E. Zielinski, and J. E. Craft. 2003. Intrinsic T cell defects in systemic autoimmunity. *Ann. N. Y. Acad. Sci.* 987: 60–67.
22. Crispin, J. C., S. N. Liossis, K. Kis-Toth, L. A. Lieberman, V. C. Kyttaris, Y. T. Juang, and G. C. Tsokos. 2010. Pathogenesis of human systemic lupus erythematosus : recent advances. *Trends Mol. Med.* 16: 47–57.
23. Xu, L., L. Zhang, Y. Yi, H. K. Kang, and S. K. Datta. 2004. Human lupus T cells resist inactivation and escape death by upregulating COX-2. *Nat. Med.* 10: 411–415.
24. Borlado, L. R., C. Redondo, B. Alvarez, C. Jimenez, L. M. Criado, J. Flores, M. A. Marcos, C. Martinez-A, D. Balomenos, and A. C. Carrera. 2000. Increased phosphoinositide 3-kinase activity induces a lymphoproliferative disorder and contributes to tumor generation. *FASEB J.* 14: 895–903.
25. Fruman, D. A., and G. Bismuth. 2009. Fine tuning the immune response with PI3K. *Immunol. Rev.* 228: 253–272.
26. García, Z., A. Kumar, M. Marqués, I. Cortés, and A. C. Carrera. 2006. Phosphoinositide 3-kinase controls early and late events in mammalian cell division. *EMBO J.* 25: 655–661.
27. Zhang, X., N. Tang, T. J. Hadden, and A. K. Rishi. 2011. Akt, FoxO and regulation of apoptosis. *Biochim. Biophys. Acta* 1813: 1978–1986.
28. Kok, K., B. Geering, and B. Vanhaesebroeck. 2009. Regulation of phosphoinositide 3-kinase expression in health and disease. *Trends Biochem. Sci.* 34: 115–127.
29. Okkenhaug, K., A. Bilancio, G. Farjot, H. Priddle, S. Sancho, E. Peskett, W. Pearce, S. E. Meek, A. Salpekar, M. D. Waterfield, et al. 2002. Impaired B and T cell antigen receptor signaling in p110delta PI 3-kinase mutant mice. *Science* 297: 1031–1034.
30. Ali, K., A. Bilancio, M. Thomas, W. Pearce, A. M. Gilfillan, C. Tkaczyk, N. Kuehn, A. Gray, J. Giddings, E. Peskett, et al. 2004. Essential role for the p110δ phosphoinositide 3-kinase in the allergic response. *Nature* 431: 1007–1011.
31. Hirsch, E., V. L. Katanaev, C. Garlanda, O. Azzolino, L. Pirola, L. Silengo, S. Sozzani, A. Mantovani, F. Altruda, and M. P. Wymann. 2000. Central role for G protein-coupled PI3K in inflammation. *Science* 287: 1049–1053.
32. Alcázar, I., M. Marqués, A. Kumar, E. Hirsch, M. Wymann, A. C. Carrera, and D. F. Barber. 2007. Phosphoinositide 3-kinase gamma participates in T cell receptor-induced cell activation. *J. Exp. Med.* 204: 2977–2987.
33. Di Cristofano, A., P. Kotsi, Y. F. Peng, C. Cordon-Cardo, K. B. Elkon, and P. P. Pandolfi. 1999. Impaired Fas response and autoimmunity in Pten+/- mice. *Science* 285: 2122–2125.
34. Barber, D. F., A. Bartolomé, C. Hernandez, J. M. Flores, C. Redondo, C. Fernandez-Arias, M. Camps, T. Rückle, M. K. Schwarz, S. Rodríguez, et al. 2005. PI3Kgamma inhibition blocks glomerulonephritis and extends lifespan in a mouse model of systemic lupus. *Nat. Med.* 11: 933–935.
35. Barber, D. F., A. Bartolomé, C. Hernandez, J. M. Flores, C. Fernandez-Arias, L. Rodríguez-Borlado, E. Hirsch, M. Wymann, D. Balomenos, and A. C. Carrera. 2006. Class IB-phosphatidylinositol 3-kinase (PI3K) deficiency ameliorates IA-PI3K-induced systemic lupus but not T cell invasion. *J. Immunol.* 176: 589–593.
36. Suárez-Fueyo, A., D. F. Barber, J. Martínez-Ara, A. C. Zea-Mendoza, and A. C. Carrera. 2011. Enhanced phosphoinositide 3-kinase δ activity is a frequent event in systemic lupus erythematosus that confers resistance to activation-induced T cell death. *J. Immunol.* 187: 2376–2385.
37. Singer, G. G., A. C. Carrera, A. Marshak-Rothstein, C. Martínez, and A. K. Abbas. 1994. Apoptosis, Fas and systemic autoimmunity: the MRL-lpr/lpr model. *Curr. Opin. Immunol.* 6: 913–920.
38. Guillou, H., C. Lécureuil, K. E. Anderson, S. Suire, G. J. Ferguson, C. D. Ellson, A. Gray, N. Divecha, P. T. Hawkins, and L. R. Stephens. 2007. Use of the GRP1

PH domain as a tool to measure the relative levels of PtdIns(3,4,5)P3 through a protein-lipid overlay approach. *J. Lipid Res.* 48: 726–732.
39. Fabian, M. A., W. H. Biggs, III, D. K. Treiber, C. E. Atteridge, M. D. Azimioara, M. G. Benedetti, T. A. Carter, P. Ciceri, P. T. Edeen, M. Floyd, et al. 2005. A small molecule-kinase interaction map for clinical kinase inhibitors. *Nat. Biotechnol.* 23: 329–336.
40. Lannutti, B. J., S. A. Meadows, S. E. Herman, A. Kashishian, B. Steiner, A. J. Johnson, J. C. Byrd, J. W. Tyner, M. M. Loriaux, M. Deininger, et al. 2011. CAL-101, a p110delta selective phosphatidylinositol-3-kinase inhibitor for the treatment of B-cell malignancies, inhibits PI3K signaling and cellular viability. *Blood* 117: 591–604.
41. Manzanero, S. 2012. Generation of mouse bone marrow-derived macrophages. *Methods Mol. Biol.* 844: 177–181.
42. Hotary, K., X. Y. Li, E. Allen, S. L. Stevens, and S. J. Weiss. 2006. A cancer cell metalloprotease triad regulates the basement membrane transmigration program. *Genes Dev.* 20: 2673–2686.
43. Camps, M., T. Rückle, H. Ji, V. Ardissone, F. Rintelen, J. Shaw, C. Ferrandi, C. Chabert, C. Gillieron, B. Françon, et al. 2005. Blockade of PI3Kgamma suppresses joint inflammation and damage in mouse models of rheumatoid arthritis. *Nat. Med.* 11: 936–943.
44. Gopal, A. K., B. S. Kahl, S. de Vos, N. D. Wagner-Johnston, S. J. Schuster, W. J. Jurczak, I. W. Flinn, C. R. Flowers, P. Martin, A. Viardot, et al. 2014. PI3Kδ inhibition by idelalisib in patients with relapsed indolent lymphoma. *N. Engl. J. Med.* 370: 1008–1018.
45. Shugg, R. P., A. Thomson, N. Tanabe, A. Kashishian, B. H. Steiner, K. D. Puri, A. Pereverzev, B. J. Lannutti, F. R. Jirik, S. J. Dixon, and S. M. Sims. 2013. Effects of isoform-selective phosphatidylinositol 3-kinase inhibitors on osteoclasts: actions on cytoskeletal organization, survival, and resorption. *J. Biol. Chem.* 288: 35346–35357.
46. Sadhu, C., B. Masinovsky, K. Dick, C. G. Sowell, and D. E. Staunton. 2003. Essential role of phosphoinositide 3-kinase delta in neutrophil directional movement. *J. Immunol.* 170: 2647–2654.
47. Foukas, L. C., M. Claret, W. Pearce, K. Okkenhaug, S. Meek, E. Peskett, S. Sancho, A. J. Smith, D. J. Withers, and B. Vanhaesebroeck. 2006. Critical role for the p110alpha phosphoinositide-3-OH kinase in growth and metabolic regulation. *Nature* 441: 366–370.
48. Jia, S., Z. Liu, S. Zhang, P. Liu, L. Zhang, S. H. Lee, J. Zhang, S. Signoretti, M. Loda, T. M. Roberts, and J. J. Zhao. 2008. Essential roles of PI(3)K-p110β in cell growth, metabolism and tumorigenesis. *Nature* 454: 776–779.
49. Laffargue, M., R. Calvez, P. Finan, A. Trifilieff, M. Barbier, F. Altruda, E. Hirsch, and M. P. Wymann. 2002. Phosphoinositide 3-kinase gamma is an essential amplifier of mast cell function. *Immunity* 16: 441–451.
50. Weening, J. J., V. D. D'Agati, M. M. Schwartz, S. V. Seshan, C. E. Alpers, G. B. Appel, J. E. Balow, J. A. Bruijn, T. Cook, F. Ferrario, et al. 2004. The classification of glomerulonephritis in systemic lupus erythematosus revisited. *J. Am. Soc. Nephrol.* 15: 241–250.
51. Crispin, J. C., M. Oukka, G. Bayliss, R. A. Cohen, C. A. Van Beek, I. E. Stillman, V. C. Kyttaris, Y. T. Juang, and G. C. Tsokos. 2008. Expanded double negative T cells in patients with systemic lupus erythematosus produce IL-17 and infiltrate the kidneys. *J. Immunol.* 181: 8761–8766.
52. Horwitz, D. A. 2008. Regulatory T cells in systemic lupus erythematosus: past, present and future. *Arthritis Res. Ther.* 10: 227.
53. Patton, D. T., O. A. Garden, W. P. Pearce, L. E. Clough, C. R. Monk, E. Leung, W. C. Rowan, S. Sancho, L. S. Walker, B. Vanhaesebroeck, and K. Okkenhaug. 2006. Cutting edge: the phosphoinositide 3-kinase p110 delta is critical for the function of CD4+CD25+Foxp3+ regulatory T cells. *J. Immunol.* 177: 6598–6602.
54. Lee, K. Y., F. D'Acquisto, M. S. Hayden, J. H. Shim, and S. Ghosh. 2005. PDK1 nucleates T cell receptor-induced signaling complex for NF-kappaB activation. *Science* 308: 114–118.
55. Chen, C., L. C. Edelstein, and C. Gélinas. 2000. The Rel/NF-kappaB family directly activates expression of the apoptosis inhibitor Bcl-x(L). *Mol. Cell. Biol.* 20: 2687–2695.
56. Waiczies, S., A. Weber, J. D. Lünemann, O. Aktas, R. Zschenderlein, and F. Zipp. 2002. Elevated Bcl-X(L) levels correlate with T cell survival in multiple sclerosis. *J. Neuroimmunol.* 126: 213–220.
57. Choi, M. S., M. Holmann, C. J. Atkins, and G. G. Klaus. 1996. Expression of bcl-x during mouse B cell differentiation and following activation by various stimuli. *Eur. J. Immunol.* 26: 676–682.
58. Soond, D. R., E. Bjørgo, K. Moltu, V. Q. Dale, D. T. Patton, K. M. Torgersen, F. Galleway, B. Twomey, J. Clark, J. S. Gaston, et al. 2010. PI3K p110δ regulates T-cell cytokine production during primary and secondary immune responses in mice and humans. *Blood* 115: 2203–2213.
59. Sanchez-Niño, M. D., A. Benito-Martin, S. Gonçalves, A. B. Sanz, A. C. Ucero, M. C. Izquierdo, A. M. Ramos, S. Berzal, R. Selgas, M. Ruiz-Ortega, et al. 2010. TNF superfamily: a growing saga of kidney injury modulators. *Mediators Inflamm.* 2010. 10.1155/2010/182958.
60. De Rycke, L., D. Baeten, D. Foell, E. Kruithof, E. M. Veys, J. Roth, and F. De Keyser. 2005. Differential expression and response to anti-TNFalpha treatment of infiltrating versus resident tissue macrophage subsets in autoimmune arthritis. *J. Pathol.* 206: 17–27.
61. Berndt, A., S. Miller, O. Williams, D. D. Le, B. T. Houseman, J. I. Pacold, F. Gorrec, W.-C. Hon, Y. Liu, C. Rommel, et al. 2010. The p110d crystal structure uncovers mechanisms for selectivity and potency of novel PI(3)K inhibitors. *Nat. Chem. Biol.* 6: 117–124.
62. Angulo, I., O. Vadas, F. Garçon, E. Banham-Hall, V. Plagnol, T. R. Leahy, H. Baxendale, T. Coulter, J. Curtis, C. Wu, et al. 2013. Phosphoinositide 3-kinase δ gene mutation predisposes to respiratory infection and airway damage. *Science* 342: 866–871.
63. Lucas, C. L., H. S. Kuehn, F. Zhao, J. E. Niemela, E. K. Deenick, U. Palendira, D. T. Avery, L. Moens, J. L. Cannons, M. Biancalana, et al. 2014. Dominant-activating germline mutations in the gene encoding the PI(3)K catalytic subunit p110δ result in T cell senescence and human immunodeficiency. *Nat. Immunol.* 15: 88–97.
64. Clayton, E., G. Bardi, S. E. Bell, D. Chantry, C. P. Downes, A. Gray, L. A. Humphries, D. Rawlings, H. Reynolds, E. Vigorito, and M. Turner. 2002. A crucial role for the p110delta subunit of phosphatidylinositol 3-kinase in B cell development and activation. *J. Exp. Med.* 196: 753–763.
65. Haylock-Jacobs, S., I. Comerford, M. Bunting, E. Kara, S. Townley, M. Klingler-Hoffmann, B. Vanhaesebroeck, K. D. Puri, and S. R. McColl. 2011. PI3Kδ drives the pathogenesis of experimental autoimmune encephalomyelitis by inhibiting effector T cell apoptosis and promoting Th17 differentiation. *J. Autoimmun.* 36: 278–287.
66. Okkenhaug, K., D. T. Patton, A. Bilancio, F. Garçon, W. C. Rowan, and B. Vanhaesebroeck. 2006. The p110delta isoform of phosphoinositide 3-kinase controls clonal expansion and differentiation of Th cells. *J. Immunol.* 177: 5122–5128.
67. Ladygina, N., S. Gottipati, K. Ngo, G. Castro, J. Y. Ma, H. Banie, T. S. Rao, and W. P. Fung-Leung. 2013. PI3Kγ kinase activity is required for optimal T-cell activation and differentiation. *Eur. J. Immunol.* 43: 3183–3196.
68. Kshirsagar, S., E. Binder, M. Riedl, G. Wechselberger, E. Steichen, and M. Edelbauer. 2013. Enhanced activity of Akt in Teff cells from children with lupus nephritis is associated with reduced induction of tumor necrosis factor receptor-associated factor 6 and increased OX40 expression. *Arthritis Rheum.* 65: 2996–3006.
69. Shin, M. S., N. Lee, and I. Kang. 2011. Effector T-cell subsets in systemic lupus erythematosus: update focusing on Th17 cells. *Curr. Opin. Rheumatol.* 23: 444–448.
70. Tracey, K. J., Y. Fong, D. G. Hesse, K. R. Manogue, A. T. Lee, G. C. Kuo, S. F. Lowry, and A. Cerami. 1987. Anti-cachectin/TNF monoclonal antibodies prevent septic shock during lethal bacteraemia. *Nature* 330: 662–664.
71. Janeway, C., P. Travers, M. Walport, and J. Capra. 1999. *Immunobiology: The Immune System in Health and Disease.* Garland, New York.
72. Nechemia-Arbely, Y., D. Barkan, G. Pizov, A. Shriki, S. Rose-John, E. Galun, and J. H. Axelrod. 2008. IL-6/IL-6R axis plays a critical role in acute kidney injury. *J. Am. Soc. Nephrol.* 19: 1106–1115.
73. Ji, H., F. Rintelen, C. Waltzinger, D. Bertschy Meier, A. Bilancio, W. Pearce, E. Hirsch, M. P. Wymann, T. Rückle, M. Camps, et al. 2007. Inactivation of PI3Kgamma and PI3Kdelta distorts T-cell development and causes multiple organ inflammation. *Blood* 110: 2940–2947.
74. Winkler, D. G., K. L. Faia, J. P. DiNitto, J. A. Ali, K. F. White, E. E. Brophy, M. M. Pink, J. L. Proctor, J. Lussier, C. M. Martin, et al. 2013. PI3K-δ and PI3K-γ inhibition by IPI-145 abrogates immune responses and suppresses activity in autoimmune and inflammatory disease models. *Chem. Biol.* 20: 1364–1374.
75. Maxwell, M. J., E. Tsantikos, A. M. Kong, B. Vanhaesebroeck, D. M. Tarlinton, and M. L. Hibbs. 2012. Attenuation of phosphoinositide 3-kinase δ signaling restrains autoimmune disease. *J. Autoimmun.* 38: 381–391.
76. Wang, Y., L. Zhang, P. Wei, H. Zhang, and C. Liu. 2014. Inhibition of PI3Kδ improves systemic lupus in mice. *Inflammation.* 37: 978–983.
77. Menke, J., W. A. Rabacal, K. T. Byrne, Y. Iwata, M. M. Schwartz, E. R. Stanley, A. Schwarting, and V. R. Kelley. 2009. Circulating CSF-1 promotes monocyte and macrophage phenotypes that enhance lupus nephritis. *J. Am. Soc. Nephrol.* 20: 2581–2592.
78. Menke, J., Y. Iwata, W. A. Rabacal, R. Basu, E. R. Stanley, and V. R. Kelley. 2011. Distinct roles of CSF-1 isoforms in lupus nephritis. *J. Am. Soc. Nephrol.* 22: 1821–1833.
79. Chang, Y. S., C. J. Liu, T. H. Wu, C. H. Chaou, K. C. Lin, S. M. Ou, T. J. Chen, W. S. Chen, C. T. Chou, and C. Y. Tsai. 2013. Survival analysis in systemic lupus erythematosus patients on maintenance dialysis: a nationwide population-based study in Taiwan. *Rheumatology* 52: 166–172.